

Determining Transmission Loss from Measured External and Internal Acoustic Environments

T. M. Scogin¹ and A. M. Smith²

NASA Marshall Space Flight Center, Huntsville, AL, 35812

An estimate of the internal acoustic environment in each internal cavity of a launch vehicle is needed to ensure survivability of Space Launch System (SLS) avionics. Currently, this is achieved by using the noise reduction database of heritage flight vehicles such as the Space Shuttle and Saturn V for liftoff and ascent flight conditions. Marshall Space Flight Center (MSFC) is conducting a series of transmission loss tests to verify and augment this method. For this test setup, an aluminum orthogrid curved panel representing 1/8th of the circumference of a section of the SLS main structure was mounted in between a reverberation chamber and an anechoic chamber. Transmission loss was measured across the panel using microphones. Data measured during this test will be used to estimate the internal acoustic environments for several of the SLS launch vehicle internal spaces.

Nomenclature

SPL	= Sound Pressure Level
dB	= decibels
OASPL	= Overall Sound Pressure Level
Hz	= frequency (cycles per second)
TL	= Transmission Loss
NR	= Noise Reduction
L_1	= mean sound pressure level in source room
L_2	= mean sound pressure level in receiving room
S	= partition area
A	= room absorption, energy loss at all room surfaces

I. Introduction

Launch vehicles are subject to extremely high Sound Pressure Levels (SPL) from acoustics generated by the vehicle’s propulsion system as well as from aero-fluctuating pressures during liftoff and ascent. These SPLs interact with the vehicle panels and cause the structure to vibrate which can be harmful to vital flight hardware mounted internally to individual vehicle panels. In addition, SPLs transmit through the vehicle skin to internal cavities which excite vibration in avionics boxes directly. From Reference 1,

During October 2009, NASA’s Engineering and Safety Center (NESC) identified that the aerospace technical community did not have a standard approach to estimate:

1. Vibration environments for mass loaded vehicle panels.
2. Vibration response and interface forces for equipment mounting to vehicle panels.¹

A series of ground tests that used acoustic noise to excite a flight-like vehicle panel were conducted at Marshall Space Flight Summer (MSFC) during June and July 2012. The vehicle panel is an aluminum orthogrid curved panel that was clamped as a partition between two chambers, one a reverberation chamber and the other an anechoic

¹ Summer Intern Program 2012, Spacecraft and Vehicle Systems Department, EV31, Marshall Space Flight Center, University of Arkansas.

² Vibroacoustics Engineer, Spacecraft and Vehicle Systems Department, EV31, Marshall Space Flight Center.

chamber. The reverberation chamber contains six angled walls offset to prevent standing waves from occurring while best representing a diffuse acoustic field.

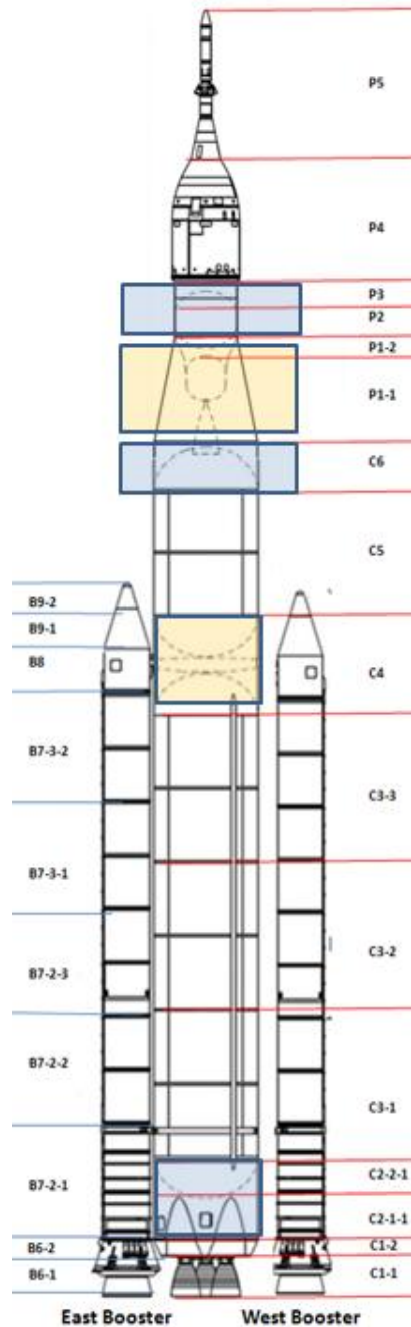


Figure 1. Depiction of the various acoustic cavities within SLS. The test panel under consideration is 1/8th the circumference of sections P3 and P2.

The air in the reverberation chamber becomes the external acoustic test environment through use of a pressurized air horn as the excitation source. The anechoic chamber is lined on all surfaces with insulated foam wedges that dampen the effect of sound and reduce echoes to eliminate excess sound readings. Using the panel, the series of

ground tests were conducted by placing microphones at equidistant locations of varying lengths including 1” and 30” from the panel on both sides and simulating liftoff and ascent acoustic environments.

The orthogrid panel represents about 1/8th or 45° of the circumference of a specific section of the upper stage of the Space Launch System (SLS) launch vehicle. Figure 1 is a representation of the SLS 10001 series divided into compartments that are expected to experience different acoustic environments during liftoff and ascent. The orthogrid panel is similar to what would be found in sections P3 and P2. The engine section tends to be significantly louder due to the sound levels emitted during activation of the engines compared to the levels in the upper stage and top of the Core Stage (CS).

II. Test Setup

Figure 2 depicts the arrangement of the test chamber with the aluminum orthogrid curved panel partitioning the two sides. It should be noted that the air horn is in actuality further to the left than depicted in Figure 2, so that the airflow that excites the panel can represent a diffuse acoustic field.

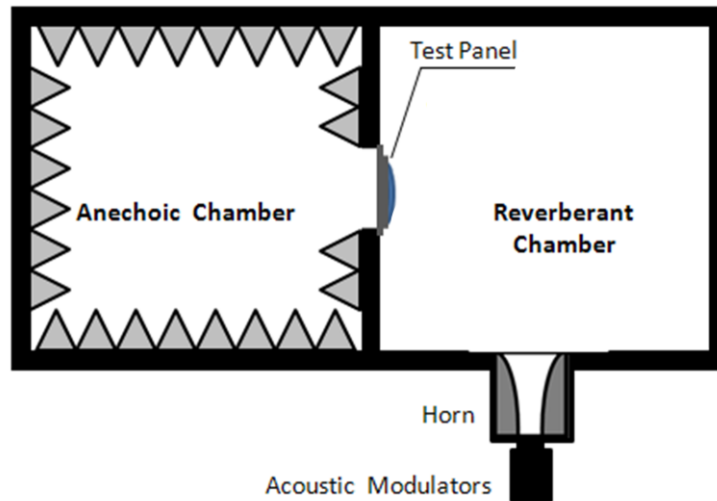


Figure 2. Test chamber setup with air horn and test article.¹

The microphones that were to be used for the tests with the horn had to be calibrated for the high intensity SPLs that they would experience in such an acoustic environment, and thus the horn was not used for the first series of test runs. A set of 8 tower speakers were selected as an alternative source for excitation of the panel. The tower speakers were lined in a row of four facing the panel, with the other four directly on top of the first row. Figure 3 represents the layout of the reverberation chamber for the panel test series with the speakers.

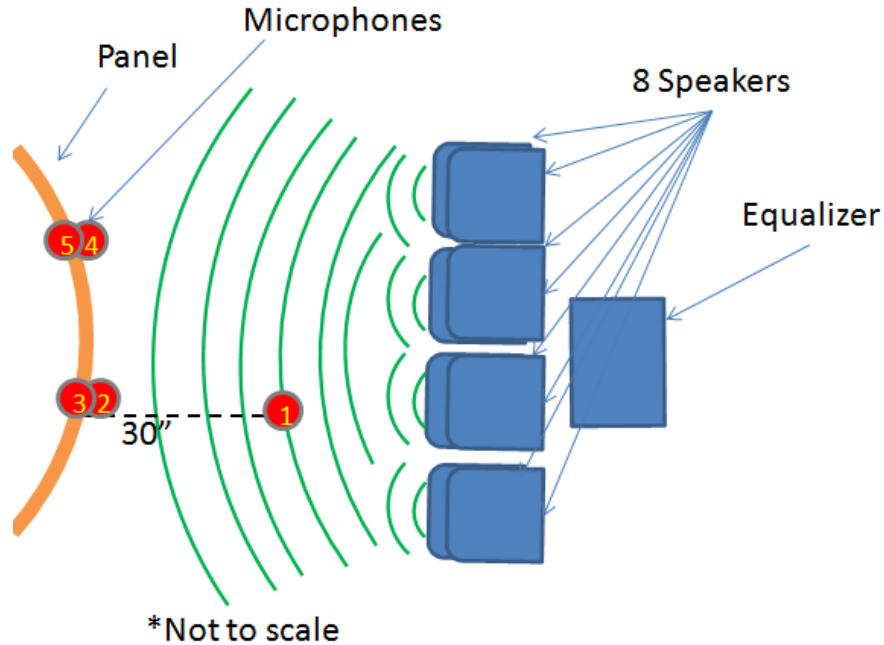


Figure 3. Test setup in reverberation chamber for bare panel speaker test.

A. Bare Panel, Speakers

The first test had no avionics mounted to the panel. Six microphones were placed on the anechoic side of the panel, and five were placed on the reverberation side. One of the microphones on the anechoic side was positioned 30 inches from the surface of the panel while the others were all 1 inch from the surface. The five microphones on the reverberation side approximately matched the spatial location of corresponding microphones on the anechoic side, including one microphone 30 inches away corresponding to the to the microphone the same distance on the reverberation side. Figure 4 depicts the locations of the microphones on both sides of the panel.

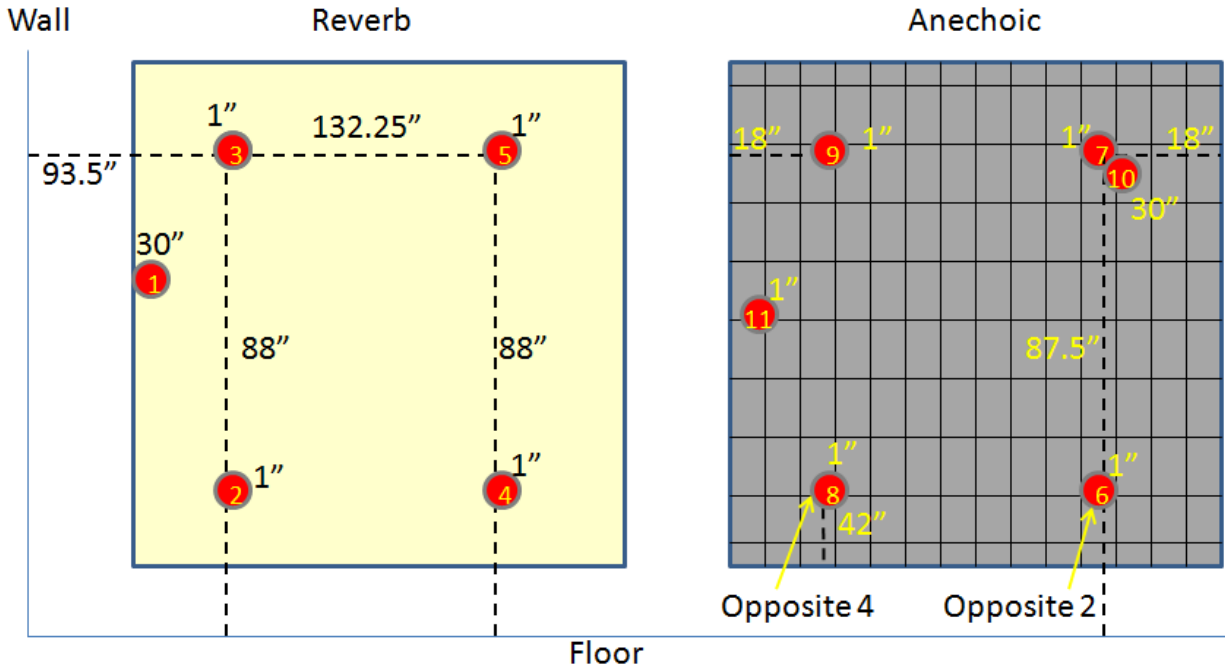


Figure 4. Microphone placements for both sides of bare panel. The number next to the microphone is the distance from the panel, and the number inside the circle is the microphone identification number. The reverberation side is covered with a layer of foam.

For this test configuration, the orthogrid panel was mounted with four rectangular brackets. These brackets have an internal cavity that is approximately 8” by 3” by 1”. They are bolted to the panel each with an aluminum plate in between the panel and bracket that closes the cavity creating an opportunity for particle damping tests. For all test configurations, bolts were tightened using a torque wrench to 145 ft-lb. The outside face of the bracket is angled so that all four create a flat surface on four edges as means to mount the desired flat object to the curved panel. To simulate the mass of flight-like avionics, a mass simulator plate weighing about 95 lb. was bolted to the four brackets. The orthogrid panel with the mass simulator and fillable brackets is one example of a “loaded panel”.

Accelerometers were also attached to the mass simulator plate in the lower left corner, center, and top right corner. However, the accelerometer data is not part of the discussion of this paper. Horizontal bars were put across the top and bottom of the tunnel space in front of the panel to allow for an attachment point for the microphones 1” from the panel. P-clamps were used to fix the microphone holders to the horizontal bars. Figure 5 is an image of the loaded panel configuration.

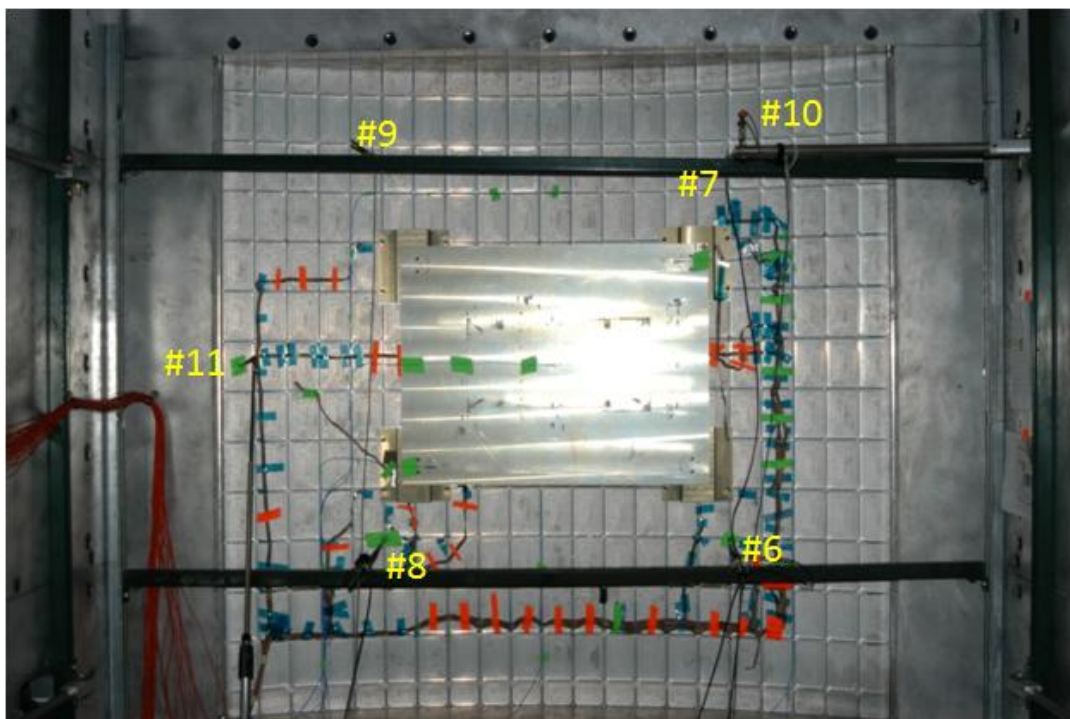


Figure 5. Microphone placements for anechoic side of the loaded panel. *Microphone 10 is located 30” away from the panel. Microphone 11 was mounted on a tripod and placed 1” away from the panel.*

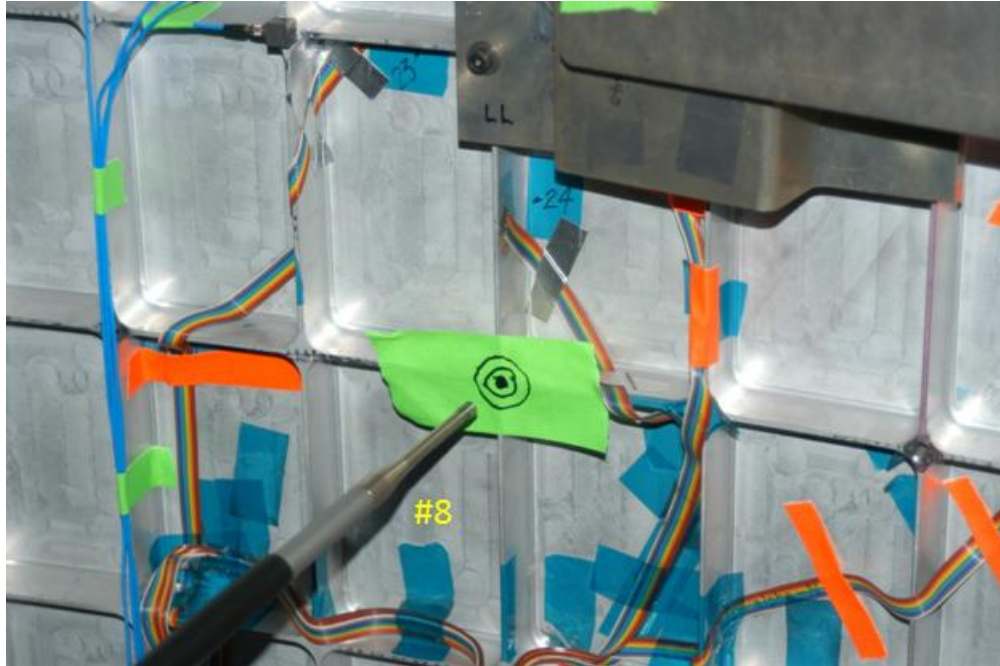


Figure 6. Close-up view of Microphone 8 placement for anechoic side of the loaded panel configuration.

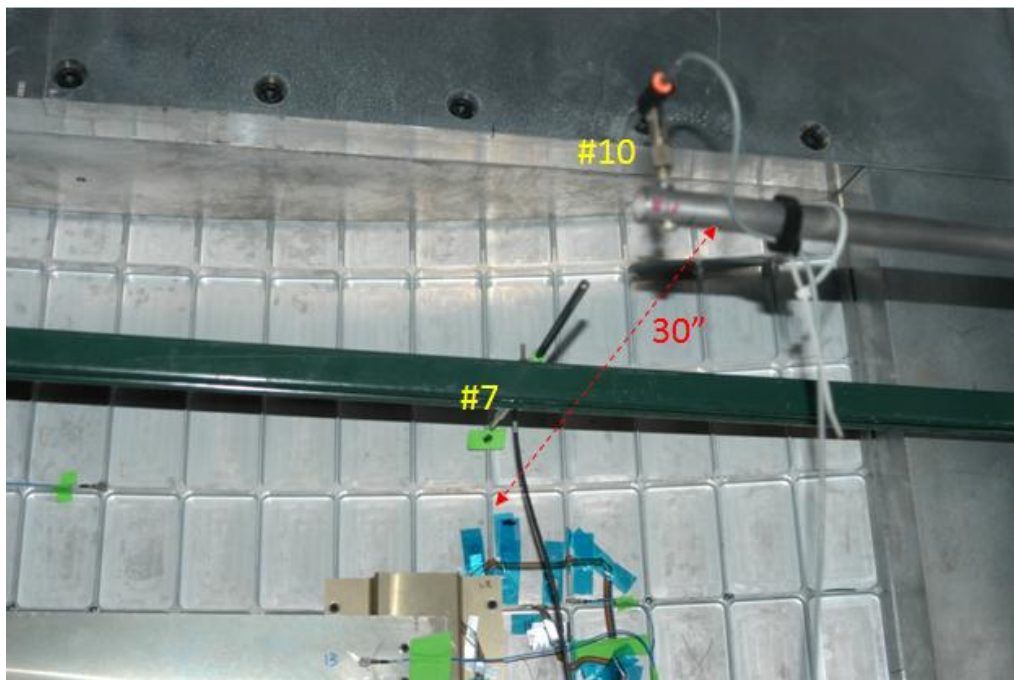


Figure 7. Microphone 10 was placed 30" away from the test panel.

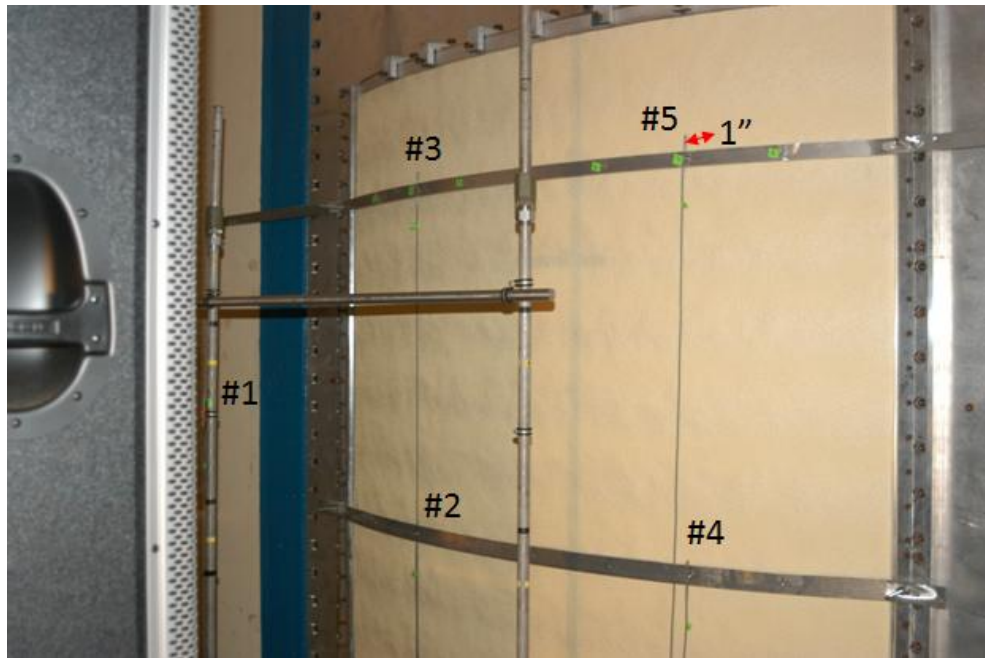


Figure 8. Microphone placements on reverberant side of panel. *Microphone 1 is 30" away; all of the other microphones located 1" away from the test panel. The edge of one of the 8 tower speakers is on the left.*

For the first particle damping test, the goal was to see the damping effect and thus the transmission loss of a simple loaded panel with no particles. For the second particle damping test, the mass simulator plate was taken off of the brackets. Each bracket was filled 50% of the total cavity volume using a funnel with small tungsten spheres to test for possible damping effects due to random vibration. Tungsten was selected for its high density compared to similar metals. The same test was repeated for a tungsten particle fill level of 90%.

III. Room Modes, Speakers

A test was run using the 8 stacked tower speakers with a new microphone and speaker setup. The goal of the test was to record the different room modes. First, the speakers were moved to the corner of the room in an attempt to excite the modes of the room. This was also achieved by placing microphones fastened to tripods in the reverberation chamber spread throughout the room at varying heights. Figure 9 depicts the reverberation chamber setup for this test.

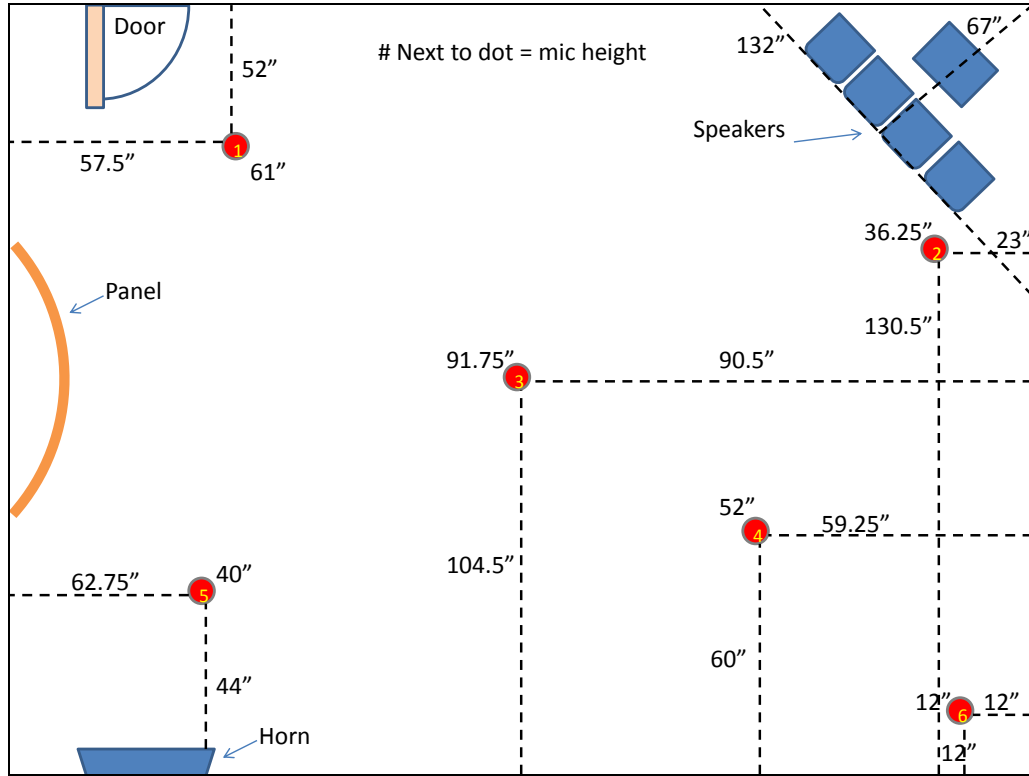


Figure 9. Microphone placements on reverberant side of panel for room modes test. Horizontal and vertical distances shown are from microphone to wall. Number adjacent to microphone is the microphone height from floor.

Figures 10 and 11 are images showing the tripods and speakers in the reverberant side of the chamber for the room modes test.

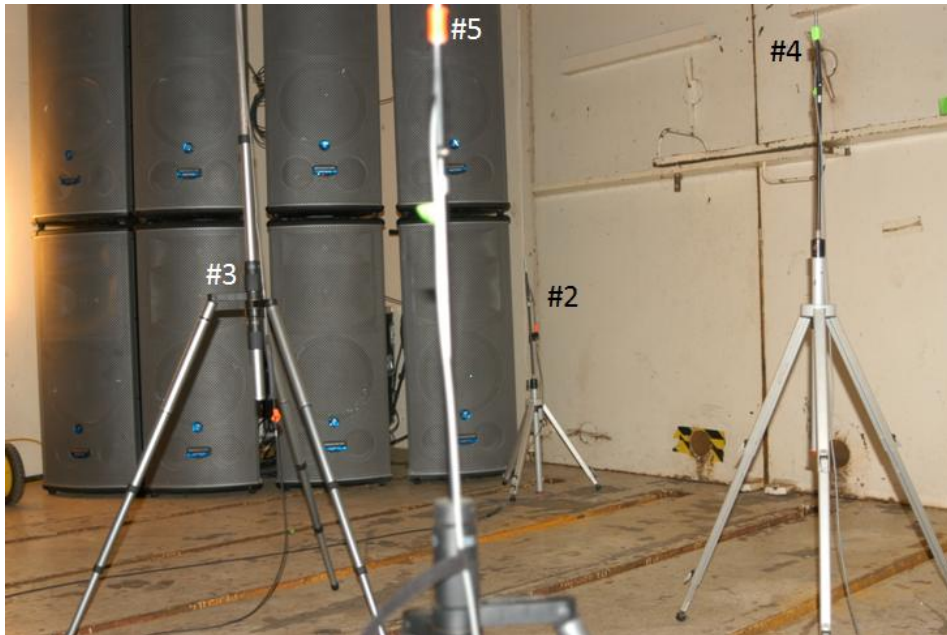


Figure 10. Tower speakers and microphone placements on reverb side for room modes test.

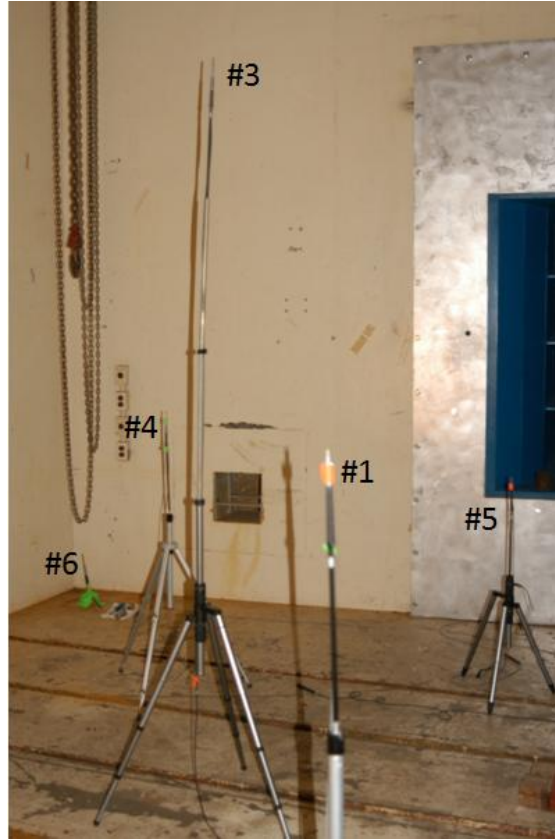


Figure 11. Tripod placements for microphones in reverb chamber for room modes test.

The microphones attached 1" from the surface of the panel on the reverberant side were also rearranged for the room modes test. Figure 12 identifies the room modes microphone configuration.

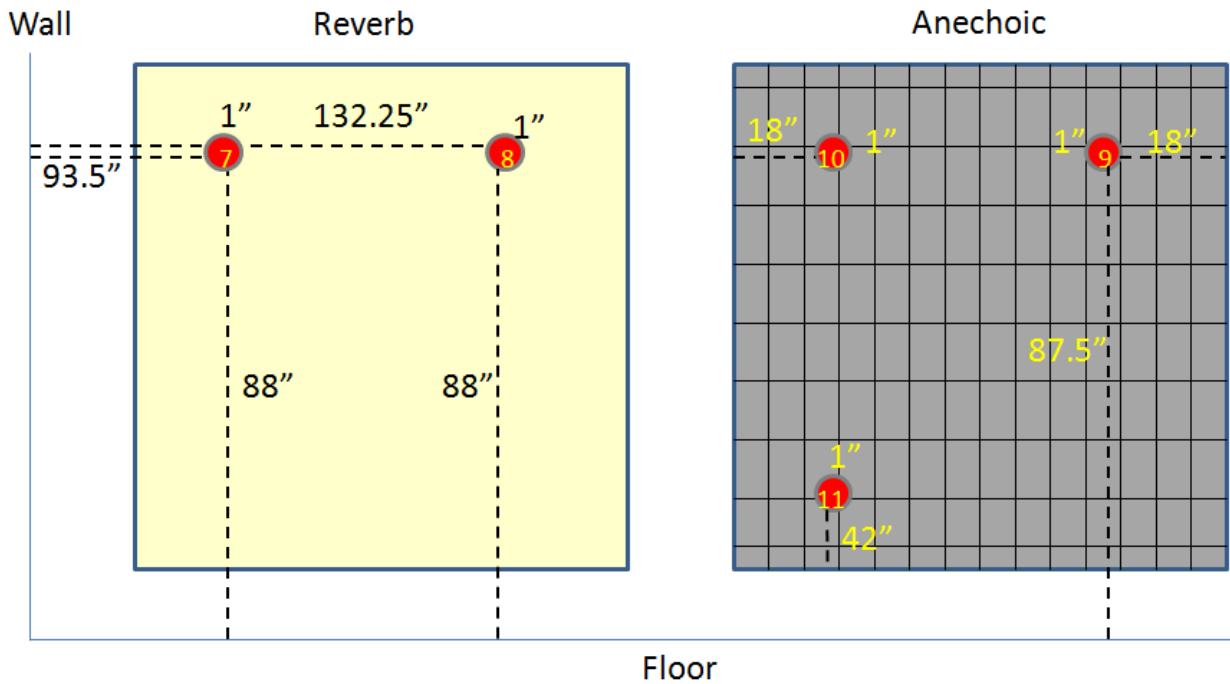


Figure 12. Microphone placements on both sides of panel for room modes test.

Figure 13 below shows an image of the anechoic side of the orthogrid panel microphone setup for the room modes test. Figure 14 shows the same for the reverberant side.

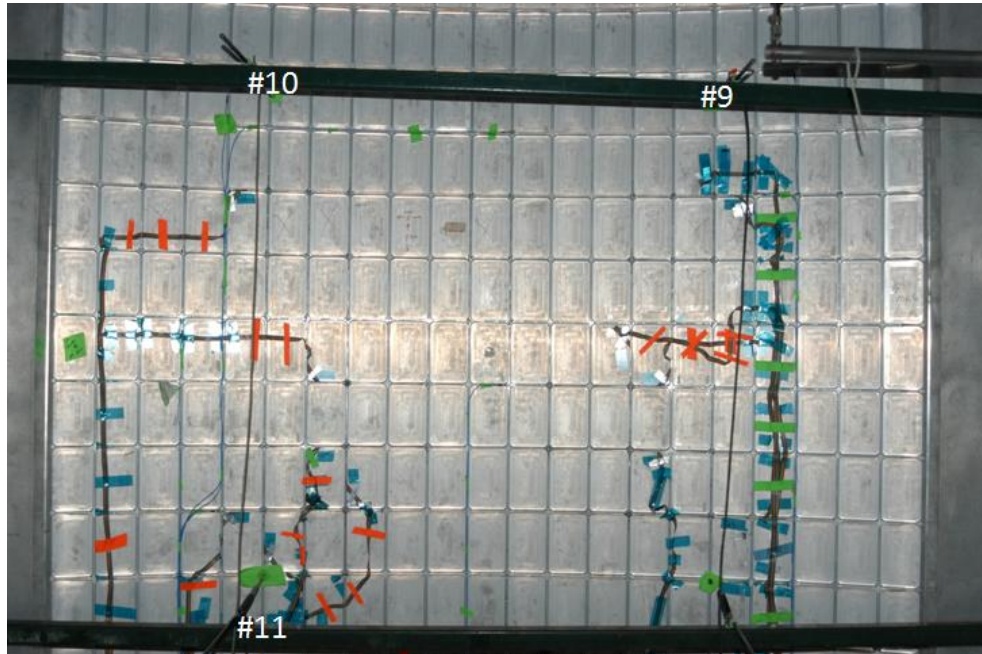


Figure 13. Microphone placements on anechoic side for room modes test. *Microphones 1" away from panel.*



Figure 14. Microphone placements on reverberant side, room modes test. *Microphones 1" away from panel.*

A. Bare Panel, Speakers

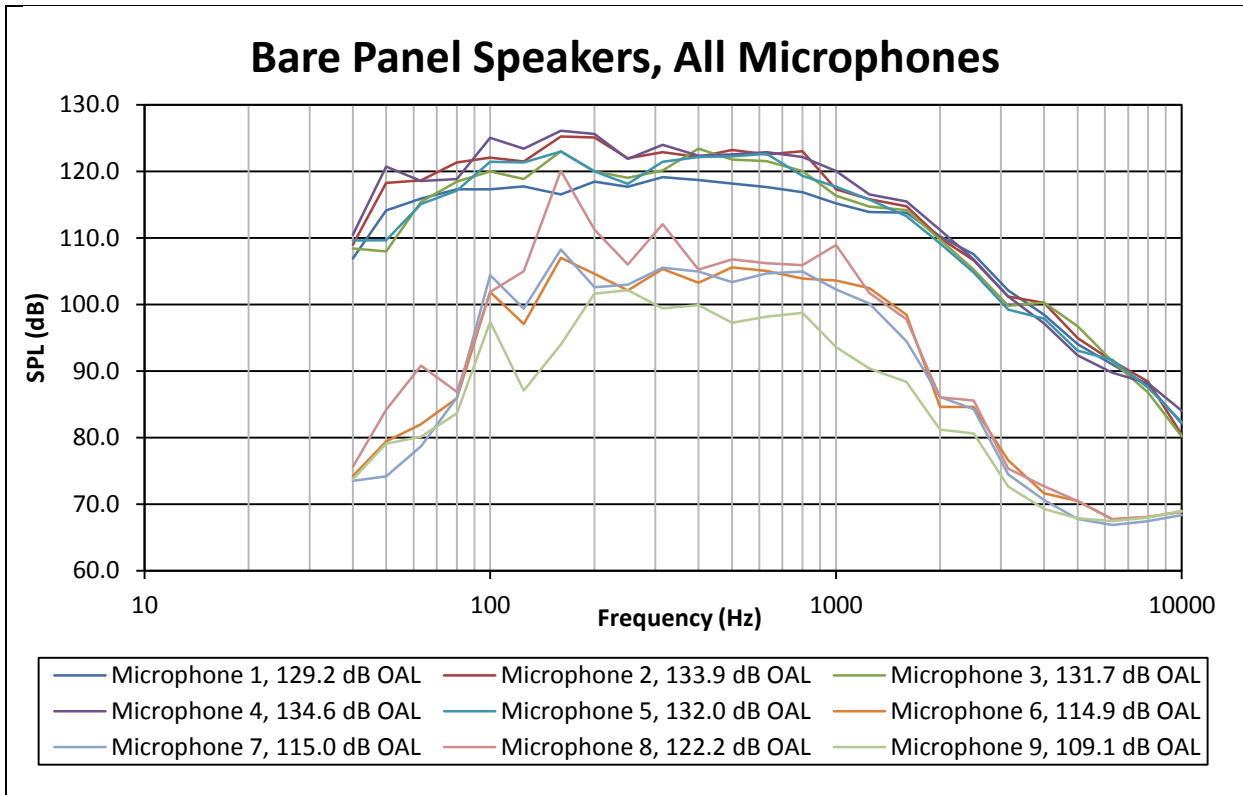


Figure 15. Plot of bare panel microphone SPL over frequency using speakers.

According to Figure 15, it is observed that microphone 8 encounters a significant spike in SPL at approximately 106 Hz and appears to become louder than the reading for microphone 1, which is located in the reverberation chamber. This is a curious and unexpected observation that may be due to a loose microphone or bolt. The two groups of microphones that trend together can be clearly observed especially in the higher frequency band range. As expected, the group in the upper SPL range match the microphones identified as those in the louder reverberation side from Figure 4, and similarly the group in the lower SPL range match the microphones in the quieter anechoic side. Another unexpected observation is the reading for microphone 9. At approximately 104 Hz, microphone 9 takes a surprisingly sharp decrease in SPL and then increases back to more expected values.

B. Loaded Panel, Speakers

Plots for the SPL versus frequency for all microphones for tests including the loaded panel with 0% particle fill level, the loaded panel with 50% particle fill level, and the loaded panel with 90% particle fill level can be found in the Appendix.

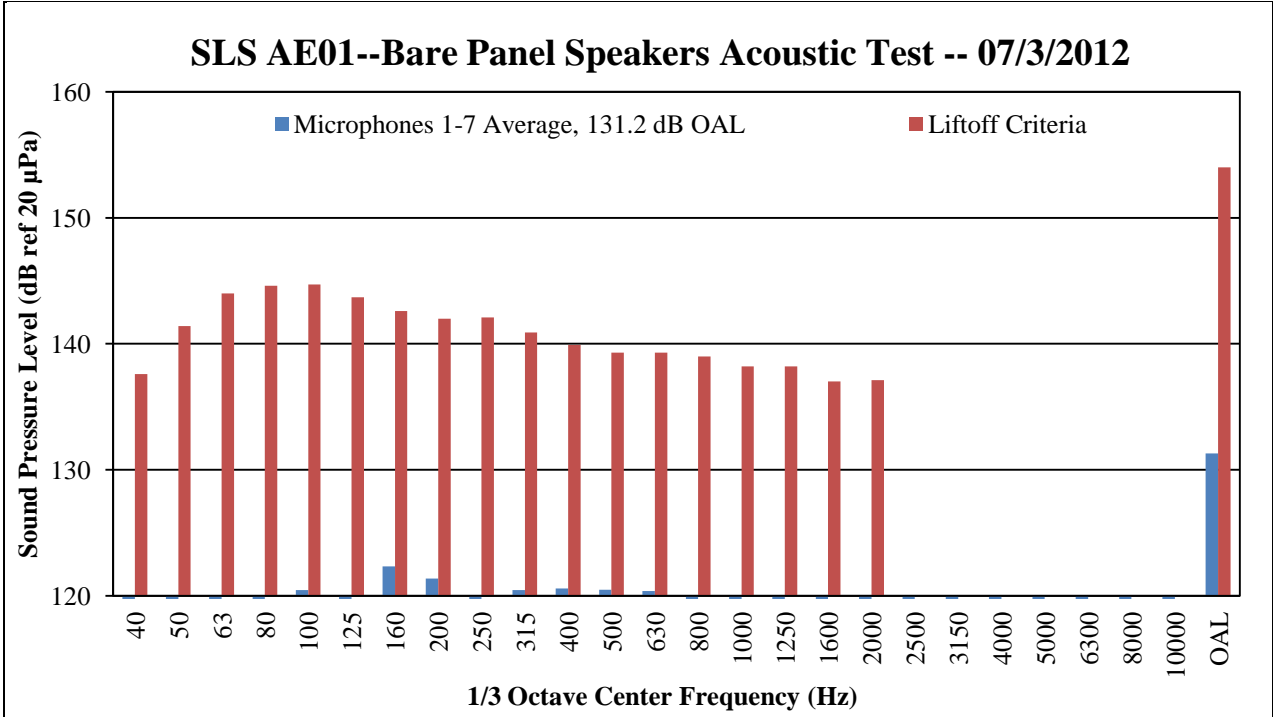


Figure 16. Bare panel microphone OASPL average compared to Liftoff Criteria.

C. Room Modes, Speakers

The plot for the SPL versus frequency for all microphones for the room modes test can be found in the Appendix.

IV. Analysis

A. Equation Discussion

The original method used for calculating the Transmission Loss (TL) involved a single equation with multiple calculations and an assumption that the receiving room was an anechoic chamber. From Reference 2,

If we begin with the assumption that the sound field in the room containing the source is perfectly diffuse, then the intensity per unit area incident on the partition $I_1 = \langle p^2 \rangle_1 / (4\rho_0 c_0)$, where ρ_0 and c_0 are the density of air and sound speed in air, respectively, and $\langle p^2 \rangle_1$ is the mean square sound pressure level in the source room. Thus the rate of transfer of sound energy through the partition separating the two rooms is $\tau S \langle p^2 \rangle_1 / (4\rho_0 c_0)$, where τ is the transmission coefficient of the partition of area S . τ is defined as the ratio of transmitted to incident intensity. The rate of energy loss in the receiving room is given by $(d/dt) \int_{V_2} \rho_2 dV_2$, where ρ_2 is the energy density in the receiving room with volume V_2 , and is a function of position in the room. In the steady state these two rates will be equal giving rise to the equation

$$\frac{\tau S \langle p^2 \rangle_1}{4\rho_0 c_0} = \frac{d}{dt} \int_{V_2} \rho_2 dV \quad (1)$$

If we assume an exponential decay of energy in the receiving room with a time constant b , then the right-hand side of Eq. (1) becomes $b \int_{V_2} \rho_2 dV$. With the further assumption that the integral can be replaced by $V_2 \langle p^2 \rangle_2 / (\rho_0 c_0^2)$ one has

$$\tau \langle p^2 \rangle_1 / (4\rho_0 c_0) = b \langle p^2 \rangle_2 V_2 / (\rho_0 c_0^2) \quad (2)$$

Setting:

$$A = 4bV_2/c_0 \quad (3)$$

and taking logarithms, one gets the familiar equation

$$TL = L_1 - L_2 + 10 \log(S/A) \quad (4)$$

where TL = transmission loss = $10 \log_{10}(1/\tau)$; L_1 = mean sound pressure level in the source room; L_2 = mean sound pressure level in the receiving room. A is identified as the room absorption and represents energy loss at all room surfaces and throughout its volume.²

Equation (4) has been the primary equation used to calculate the TL plots with the assumption that the receiving room is an anechoic chamber. For the transmission loss calculations, the room absorption A was calculated differently than the way that Ref. 2 calculates A . Reference 2 did not specify what the time constant b referred to, so an alternative equation was selected to find A . Reference 3 was found to have a solution,

The *reverberation time* T , defined as the time required for the level of the sound to drop by 60 dB, is $T = 13.82\tau_E = 55.3V/(Ac)$. Expressing V in cubic meters, A in metric sabin, and with $c = 343$ m/s, we obtain the metric form of the *Sabine reverberation formula*,

$$T = 0.16V/A \quad (5)$$

(In English units, if V is in cubic feet, A in English sabin, and $c = 1125$ ft/s, then $T = 0.049V/A$.)³

The second form of the equation,

$$A = 0.049V/T \quad (6)$$

was used for A in the transmission loss calculation using Eq. (4). The reverberation time T at each frequency band was found by conducting a T60 time test. For both the reverberation and anechoic chambers, an average balloon was popped and the time domain of the SPL recorded to find the time that it took for the SPL to drop by 60 dB. The point of the balloon pop test is to simulate a spike in SPL and record the decay of that spike which depends on the properties of the surfaces in the room.

B. Transmission Loss

To find and plot transmission loss, the test result data was organized and used for calculations in Microsoft Excel 2010. External and internal flight environments were measured from heritage launch vehicles such as the Space Shuttle and the Saturn V during flight. Eq. (4) was used to calculate the TL, and those TL values were subtracted from the heritage external SPLs to find the internal acoustic environments for SLS. As can be seen in Eq. (6), the volume of the anechoic chamber plays a role in the calculation for TL in Eq. (4). The volume of the anechoic room was found by taking various measurements with a tape measure. The volume of the space in the room was calculated by subtracting the total volume of the insulated foam wedges from the total volume of the room as if it was empty.

The liftoff SPLs over frequency were plotted. Figure 17 below contains the external and internal SPLs that were compared for liftoff with a smoothed internal line. The process of smoothing the internal acoustic line involved using the original external line, and capturing the trend of the peaks and valleys as well as matching the envelope of the external acoustic environment. Below that, Figure 18 is a plot of the overall noise reduction (NR) as well as the plot of TL.

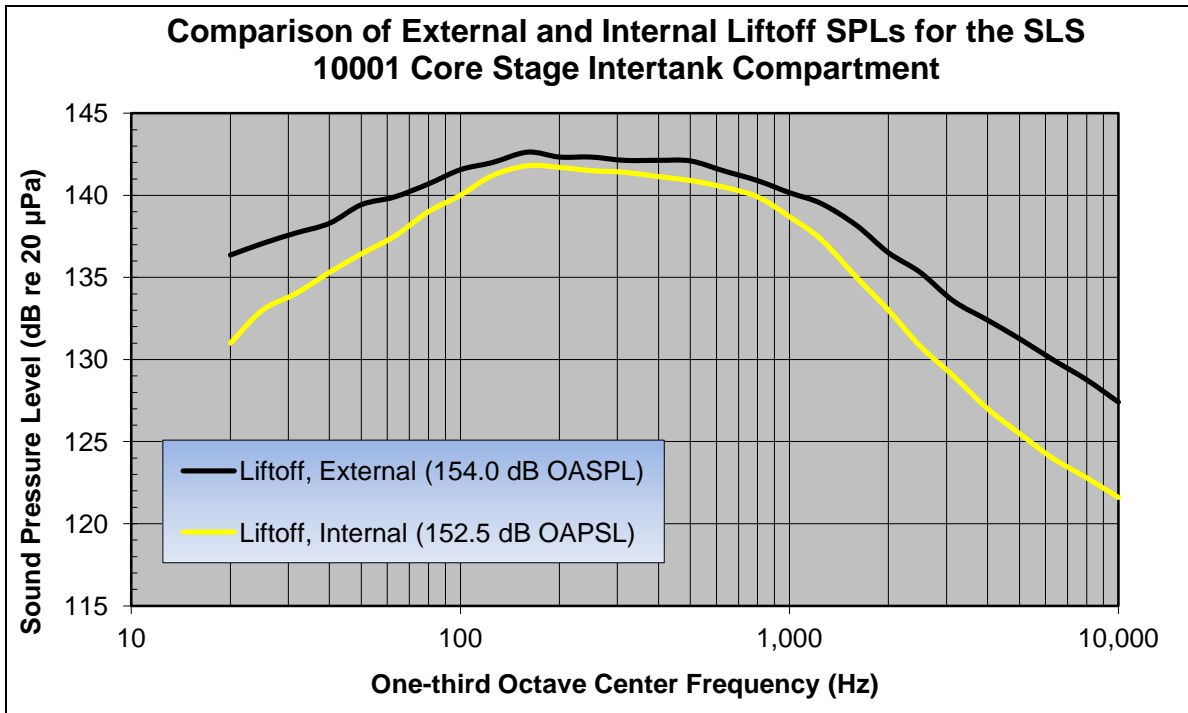


Figure 17. Smoothed plot of external and internal liftoff SPLs.

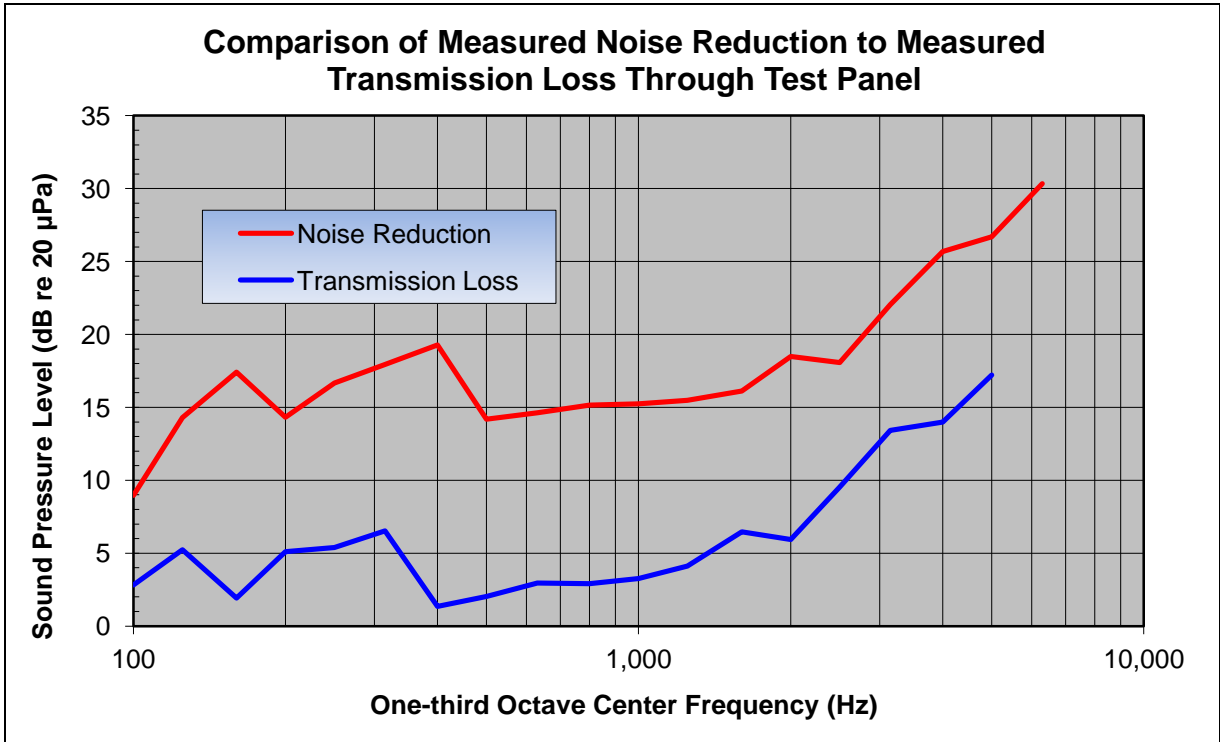


Figure 18. Plot of noise reduction and transmission loss SPLs.

V. Future Work

There is quite a bit of work to be done on this project. There is a plan in place to attach two shelves supported by four struts to the aluminum panel. Flight-like avionics will be bolted to the shelves to simulate and see the acoustic response for a possible configuration for mounting avionics within the internal cavities for SLS. It is also possible that a sample of acoustic blankets will be purchased to observe additional noise reduction across the panel. To validate the vendor’s claim of the capabilities of the blankets, the aluminum panel will be lined with these acoustic blankets and tested to see what the additional transmission loss is. Another plan for future work includes changing out the current aluminum orthogrid panel for a panel that is of the triangular isogrid pattern which is currently in place for the inner wall skin of SLS. Also, the new panel could be curved wider to better model the circumference of larger primary structure sections such as the Intertank or Engine section, sections C4 and C2 respectively on Figure 1.

VI. Conclusion

The test panel was exposed to OASPLs of about 135 dB with the 8 tower speakers, and about 160 dB with the pressured air horn. With the quieter OASPL, the orthogrid panel saw approximately 3 dB of transmission loss being tested with the speakers. With the louder OASPL of the air horn, the panel saw approximately 5 dB of transmission loss.

Appendix

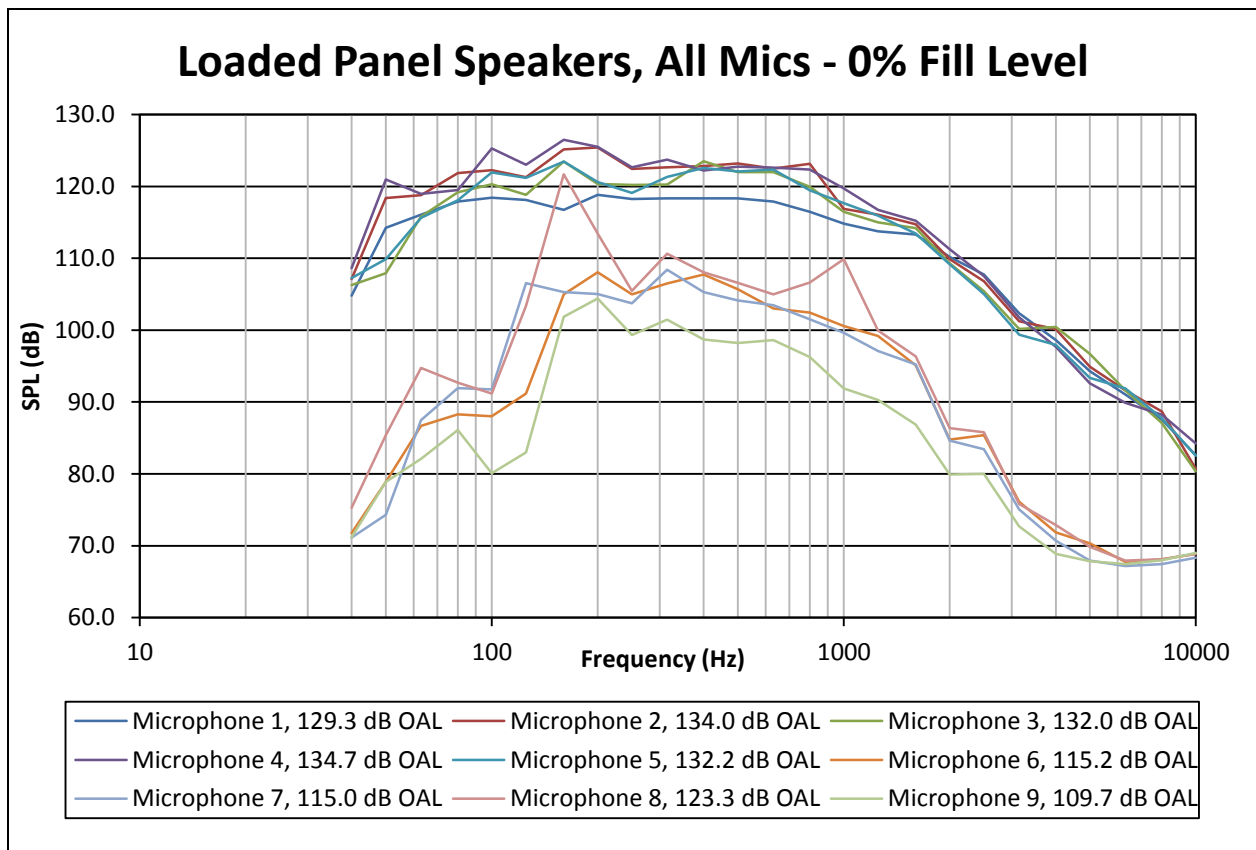


Figure 19. Plot of loaded panel microphone SPL over frequency using speakers with 0% fill level.

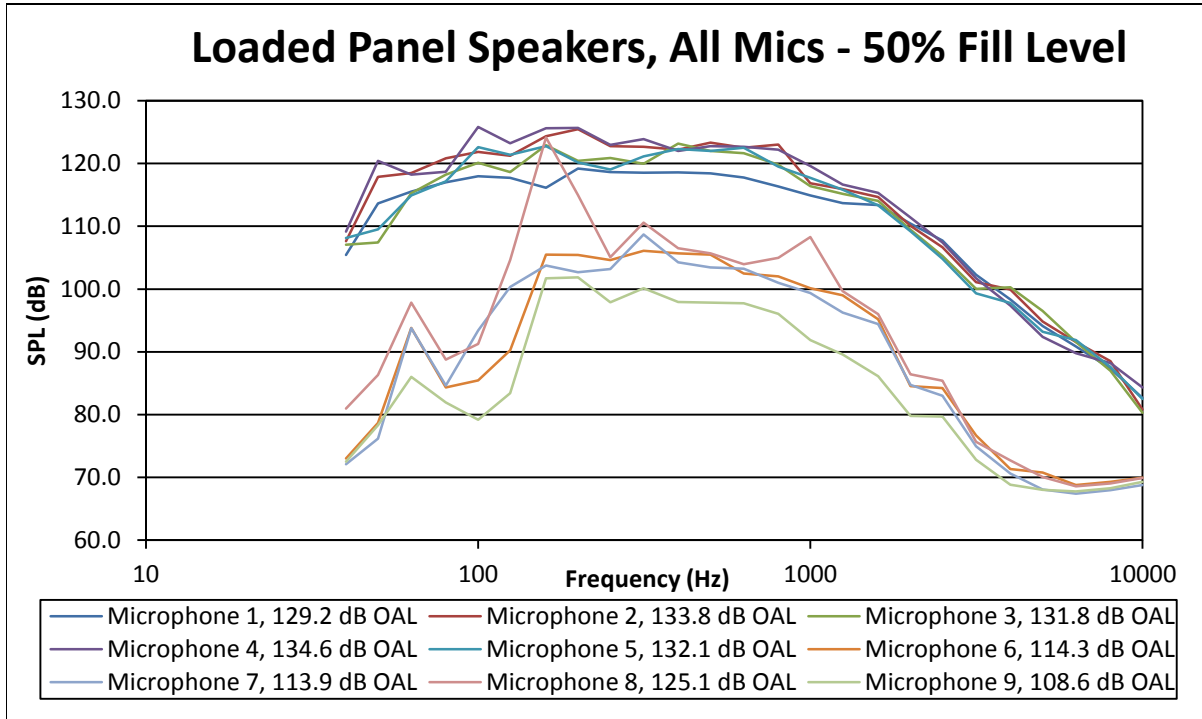


Figure 20. Plot of loaded panel microphone SPL over frequency using speakers with 50% fill level.

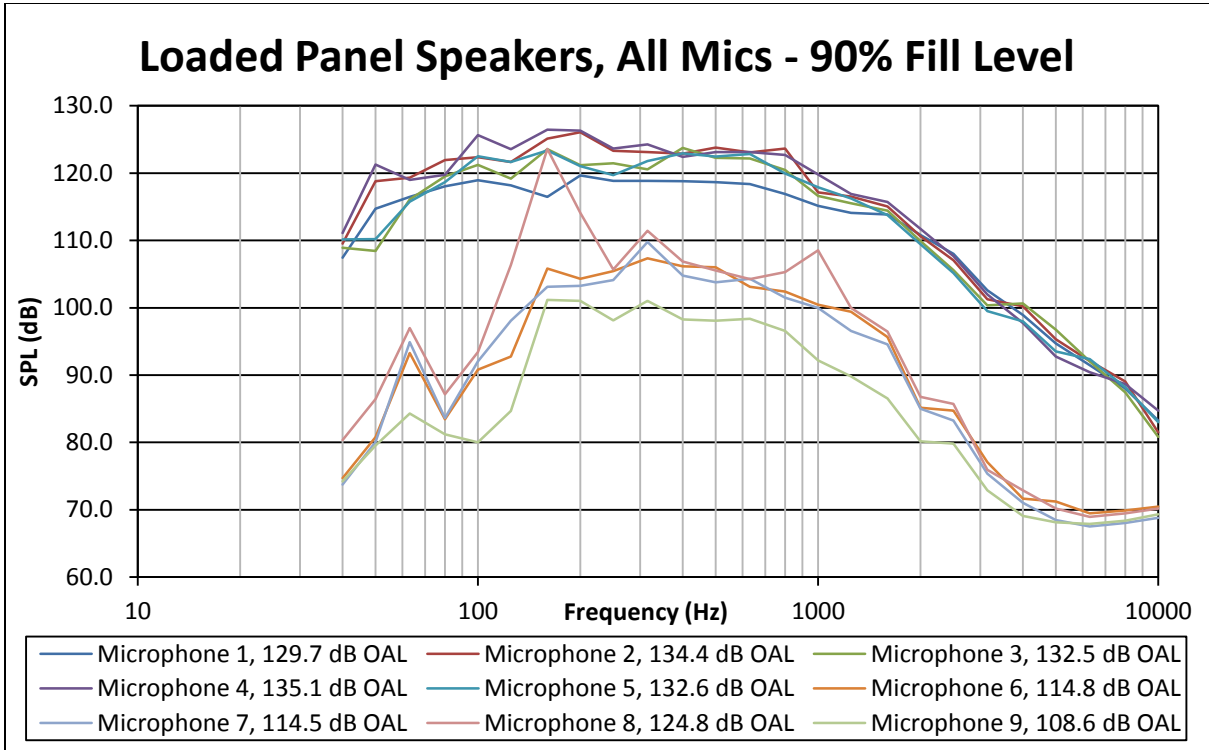


Figure 21. Plot of loaded panel microphone SPL over frequency using speakers with 90% fill level.

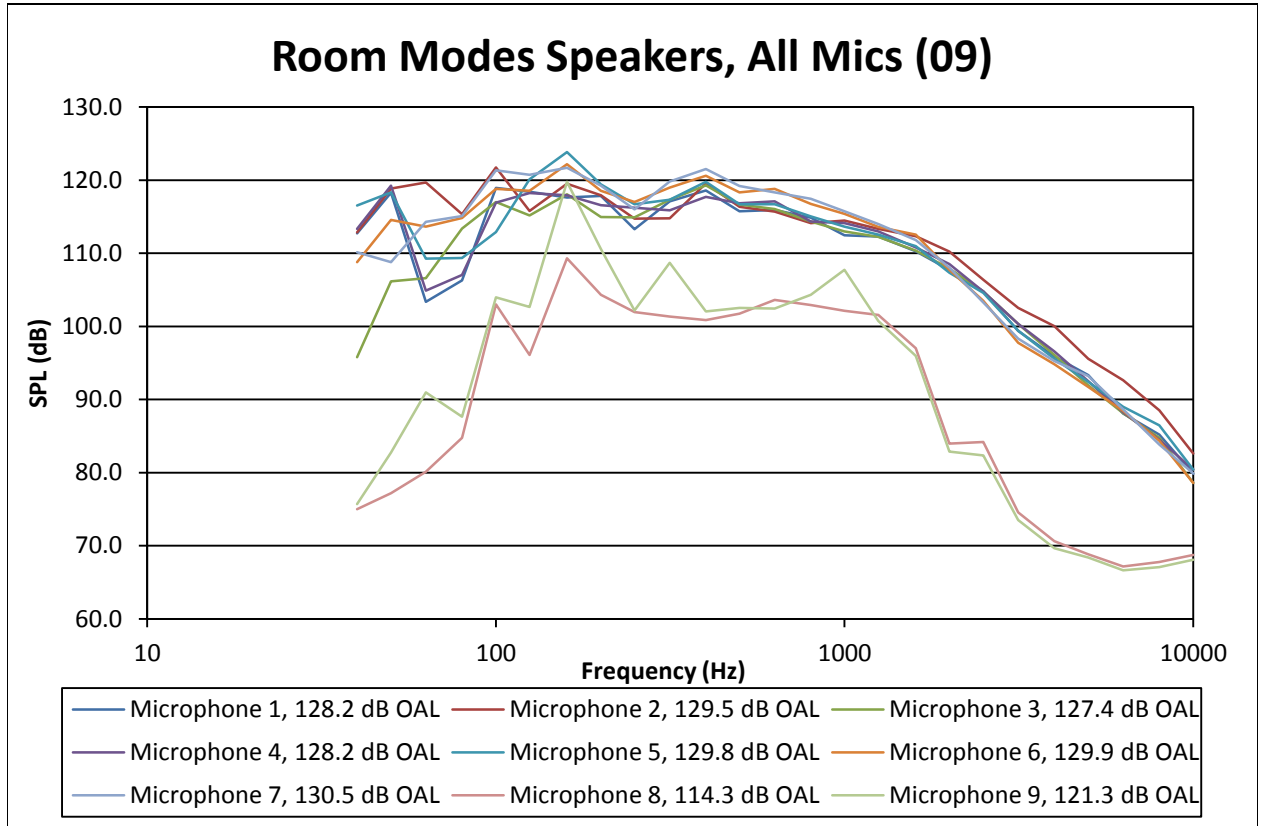


Figure 22. Plot of room modes test with microphone SPL over frequency using speakers.

Acknowledgments

T. M. Scogin thanks A. M. Smith for his invaluable help, enthusiasm, and patience throughout the duration of this project. The author also thanks Bruce LaVerde, David Teague, Steve Rodgers, and Karen Oliver for their contributions to the project. This internship was funded through the NASA Arkansas Space Grant Consortium.

References

- ¹ Phil Harrison, Andrew Smith, Bruce LaVerde, Ron Hunt, and David Teague. 2011. AD01 Ground Acoustic Development Test, Initial Assessment Report. National Aeronautics and Space Administration (NASA). Document EV31-001-RPT-2011-01. 74 p.
- ² Halliwell, R. E., and Warnock, A.C.C., “Sound Transmission Loss: Comparison of Conventional Techniques with Sound Intensity Techniques,” *Journal of Acoustical Society of America*, Vol. 77, No. 6, 1985, pp. 2096.
- ³ Kinsler, L. E., Frey, A. R., Coppens, A. B., and Sanders, J. V. *Fundamentals of Acoustics*, 4th ed., John Wiley & Sons, Inc., New Jersey, 1976, pp 33.